Fermi National Accelerator Laboratory

FERMILAB-PUB-93/142-T
BNL-49447

Higgs Bosons at the Fermilab Tevatron

A. Stange and W. Marciano

Physics Department
Brookhaven National Laboratory
Upton, NY 11973

and

S. Willenbrock*

Fermi National Accelerator Laboratory
P. O. Box 500
Batavia, IL 60510

and

Physics Department
Brookhaven National Laboratory
Upton, NY 11973

Abstract

We study the production and detection of the standard-model Higgs boson at the Fermilab Tevatron. The most promising mode is WH and ZH associated production followed by leptonic decay of the weak vector bosons and $H \to b\bar{b}$. It may be possible to detect a Higgs boson of mass $m_H = 60$–80 GeV with 1000 pb^{-1} of integrated luminosity. We also study the signature for a non-standard "bosonic" Higgs boson whose dominant decay is to two photons. A signal is easily established with 100 pb^{-1} in the WH and ZH channels, with the weak vector bosons decaying leptonically or hadronically, up to $m_H = 100$ GeV.

*Address after September 1, 1993: Department of Physics, University of Illinois, 1110 West Green Street, Urbana, Illinois 61801.

Operated by Universities Research Association Inc. under contract with the United States Department of Energy

1 Introduction

The evidence is overwhelming that the electroweak interaction is described by an $SU(2)_L \times U(1)_Y$ gauge theory, spontaneously broken to $U(1)_{EM}$. However, the precise mechanism which breaks the electroweak symmetry is unknown. The simplest mechanism is the standard Higgs model, in which the symmetry is broken by the vacuum-expectation value of a fundamental scalar field. This model predicts the existence of a scalar particle, the Higgs boson, with fixed couplings to other particles, but of unknown mass. The search for this particle constitutes the baseline in our search for phenomena associated with the electroweak-symmetry-breaking mechanism.

The current lower bound on the mass of the Higgs boson is about 60 GeV, from the process $Z \to Z^*H$ at LEP [1] (Z^* denotes a virtual Z boson). This bound is limited by statistics and backgrounds, and is unlikely to improve significantly. The next extension in reach will be provided by LEP II, beginning in 1995, which will explore up to a Higgs-boson mass of about 80 GeV via $Z^* \to ZH$ [2]. Much higher masses will be explored by the CERN Large Hadron Collider (LHC) and the U.S. Superconducting Super Collider (SSC), which can reach as high as $m_H = 800$ GeV via the processes $gg \to H$ and $V^*V^* \to H$ ($V = W, Z$) [3].

Conspicuously absent from this discussion is the Fermilab Tevatron $p\bar{p}$ collider. It is generally assumed that the Tevatron cannot probe the electroweak-symmetry-breaking mechanism. However, there are two reasons why this is an appropriate time to study the possibility of searching for the Higgs boson at the Tevatron. First, the Tevatron is operating with high luminosity, and it now seems possible that 100 pb^{-1} of integrated luminosity will be delivered to each of the two detectors by the end of 1994. Furthermore, with the Main Injector, a five-fold increase in luminosity will be obtained, yielding 1000 pb^{-1} of integrated luminosity per detector by the end of the century, and perhaps more. Second, it has been demonstrated that vertex detection is feasible in a hadron-collider environment. This allows the detection of secondary vertices from the decay of b quarks, which is vital for searching for the decay $H \to b\bar{b}$.

In Section 2 we study the production of the Higgs boson in association with a W or Z boson at the Tevatron [4]. The leptonic decay of the W or Z boson provides a trigger for the event and suppresses the backgrounds. In the mass range of interest, the standard Higgs boson decays predominantly to $b\bar{b}$, and vertex detection must be used to separate b jets from light-quark jets. This process has been extensively studied for the LHC [5] and SSC [6, 7, 8, 9, 10], but no similar study has been undertaken for the Tevatron. While the analysis is similar to that of the LHC/SSC in many respects, it differs in several important ways.

In Section 3 we discuss the search for a "bosonic" Higgs, which is a Higgs boson with ordinary coupling to weak vector bosons, but suppressed coupling to fermions. For $m_H < 100$ GeV, this Higgs boson has a significant branching ratio to two photons via a virtual W-boson loop. Its production in association with a W or Z boson yields an observable signal in both the leptonic and hadronic decay modes of the weak vector bosons with just 100 pb^{-1} of integrated luminosity. In Section 4 we summarize the conclusions of our study.

2 Standard Higgs boson

The production of the Higgs boson at the LHC/SSC has been extensively studied [3]. The same processes occur at the Tevatron, but with different relative rates. We show in Fig. 1 the total cross sections for various Higgs-boson production processes: gluon fusion via a virtual top-quark loop [11], associated production with a W or Z boson [4], weak-vector-boson fusion [12], and associated production with a $b\bar{b}$ [13] or $t\bar{t}$ [14, 15] pair ($m_t = 150$ GeV). We have included the QCD correction to the gluon-fusion cross section, which is approximately a factor of 2.2 (in the $\overline{MS}$ scheme with $\mu = m_H$) [17, 18, 19].* The QCD correction to WH/ZH production is also included; it is about +25% in the $\overline{MS}$ scheme with $\mu = M_{VH}$ [20]. The QCD correction to vector-boson fusion is only a few percent [21]. Although gluon fusion yields the largest cross section, it is relatively less important than at the LHC/SSC due to the decreased gluon luminosity at the Tevatron. The associated production with a $t\bar{t}$ pair is suppressed relative to the LHC/SSC for the same reason, especially because the top quark is relatively heavy compared with the machine energy. For this reason, associated production with a $b\bar{b}$ pair is much larger than with a $t\bar{t}$ pair, in contrast with the corresponding cross sections at the LHC/SSC.

The branching ratios of the Higgs boson to $b\bar{b}$, $c\bar{c}$, $\tau^+\tau^-$, $WW^{(*)}$, and $ZZ^{(*)}$ [22] are shown in Fig. 2. The direct production of the Higgs boson via gluon fusion, followed by $H \to b\bar{b}$ or $c\bar{c}$, is swamped by the QCD production of $b\bar{b}$ and $c\bar{c}$ pairs. Similarly, the mode $H \to WW^{(*)} \to \ell\bar{\nu}\bar{\ell}'\nu'$ is swamped by the production of real W-boson pairs. The $H \to ZZ^{(*)} \to \ell\bar{\ell}\ell'\bar{\ell}'$ or $\ell\bar{\ell}\nu\bar{\nu}$ modes yield too few events to observe.† The $H \to \tau^+\tau^-$ mode cannot be reconstructed due to the loss of the tau neutrinos [24].

Associated production with a W or Z boson is relatively more important at the Tevatron than at the LHC/SSC. The leptonic decay of the W or Z boson (including $Z \to \nu\bar{\nu}$) provides a trigger for the event, and suppresses backgrounds. It is these processes upon which we concentrate. The WH process has already been used at the Tevatron to eliminate a very light Higgs boson [25]. As we will show, at least 1000 pb^{-1} will be required to search for a more massive Higgs boson at the Tevatron. Thus we make cuts to simulate the acceptance of an upgraded CDF/D0 detector that one can envision existing by the time the Main Injector is operating.

Consider the decay of the Higgs boson to a $b\bar{b}$ pair. To suppress the Wjj and Zjj background, we must require that at least one of the jets be identified as coming from a b quark. We require $|\eta_b| < 2$ for the b and $\bar{b}$ rapidity to simulate the coverage of the vertex detector, and we further require the rapidity, transverse momentum (p_T), and isolation cuts listed in Table 1. The resulting cross sections are shown in Fig. 3, including all branching ratios ($\ell = e, \mu$). The WH process contributes to the ZH cross section when the charged lepton from the W decay is missed; the ZH process contributes only a small amount to the WH cross section, when one of the charged leptons from $Z \to \ell\bar{\ell}$ is missed.

The principal backgrounds are $Wb\bar{b}$ [15, 6, 10, 26, 27] and $Zb\bar{b}$ [26, 28], WZ [29] and ZZ [30] followed by $Z \to b\bar{b}$, and $t\bar{t}$ production. The $Wb\bar{b}$ and $Zb\bar{b}$ backgrounds are shown in

*All QCD corrections quoted in this paper are in the $\overline{MS}$ scheme, with a fixed set of next-to-leading-order parton distribution functions [16] used for the leading-order and next-to-leading-order calculations.

†This process was considered by V. Barger and T. Han in Ref. [23] at the Tevatron with $\sqrt{s} = 3.6$ TeV and 1000 pb^{-1}, with a negative conclusion.

Table 1: Acceptance cuts used in section 2 to simulate an upgraded CDF/D0 detector.

$\|\eta_b\| < 2$	$p_{Tb} > 15$ GeV
$\|\eta_\ell\| < 2.5$	$p_{T\ell} > 20$ GeV
$\not{p}_T > 20$ GeV	(for $W \to \ell\bar{\nu}, Z \to \nu\bar{\nu}$)
$\|\eta_j\| < 2.5$	$p_{Tj} > 15$ GeV
$\|\Delta R_{b\bar{b}}\| > 0.7$	$\|\Delta R_{b\ell}\| > 0.7$

Fig. 3, assuming a $b\bar{b}$ invariant-mass resolution equal to a typical two-jet invariant-mass resolution. We assume $\Delta E_j/E_j = .80/\sqrt{E_j} \oplus .05$ for the jet energy resolution, which corresponds to approximately $\Delta M_{jj}/M_{jj} = .80/\sqrt{M_{jj}} \oplus .03$ for the two-jet invariant-mass resolution. We integrate the background over an invariant-mass bin of size $\pm 2\Delta M_{jj}$ centered at m_H, which contains nearly all the signal events. The invariant-mass resolution may be degraded somewhat since about forty percent of all events have at least one neutrino from semileptonic b decay. The signal-to-background ratio is of order unity, and is better for ZH than WH because the HZZ coupling is bigger than the HWW coupling by M_Z^2/M_W^2. Recall that at the LHC/SSC the ZH signal is swamped by $gg \to Zb\bar{b}$ [6]. This is not the case at the Tevatron; $q\bar{q} \to Zb\bar{b}$ is slightly larger than $gg \to Zb\bar{b}$, due to the decreased gluon luminosity.

The background processes WZ and ZZ, with $Z \to b\bar{b}$, populate the region between about 80 and 100 GeV. The cross sections, including the QCD corrections (+33% for WZ [29], +25% for ZZ [30] in the $\overline{MS}$ scheme with $\mu = M_{VV}$), are shown in Fig. 3; they are comparable to the signal, and increase the background in this region. These backgrounds could be calibrated using the purely leptonic decays of the gauge-boson pairs.

The top quark is also a potential background. The process $t\bar{t} \to W^+W^-b\bar{b}$ mimics the WH signal if one W goes undetected. We assume a coverage for jets of $|\eta_j| < 2.5$ and $p_{Tj} > 15$ GeV, and reject events with additional jets.[‡] With this coverage, the dominant $t\bar{t}$ background occurs when the charged lepton from a W decay goes outside the coverage of the detector. We make the additional requirement that the transverse mass of the observed charged lepton plus the missing p_T be less than M_W, which is always true for the signal. This cut reduces the background by about a factor of two. This background is shown in Fig. 3(a) for $m_t = 150$ GeV; it is far less troublesome than the direct $Wb\bar{b}$ background. The top quark is also a background to the ZH signal, with $Z \to \nu\bar{\nu}$, if both W's are missed. This background is shown in Fig. 3(b); it is negligible. In both cases, the top-quark background decreases for a heavier top quark. The top-quark background is a much worse problem at the LHC/SSC.[§]

Another serious background is $Wc\bar{c}$ and $Zc\bar{c}$. Since the charm-quark lifetime is comparable to that of the bottom quark, these events can also produce a displaced vertex, and could as much as double the background. Final states with a single charm quark, such as $W^-c\bar{s}$, can also contribute to the background if only one jet is required to have a displaced

[‡]Rejecting events with additional jets decreases the signal somewhat. This reduction can be minimized by increasing the minimum p_T of the additional jets, without greatly increasing the background.

[§]The top-quark background at the SSC was considered by R. Kauffman in Ref. [9].

vertex. In Ref. [7, 8] the charm-quark background was suppressed by demanding that the b quark decay semileptonically, with lepton momentum transverse to the b jet of at least 1 GeV. Due to the modest number of signal events, one may not be able to afford such a cut at the Tevatron. Perhaps another method can be found.

One must also consider the Wjj and Zjj backgrounds, where the jets come from light quarks [31, 32, 33, 34, 35, 36, 37]. Applying the same acceptance cuts and invariant-mass resolution as before, we find that these cross sections are about one hundred times as large as the $Wb\bar{b}$ and $Zb\bar{b}$ backgrounds.[¶] Excellent light-quark-jet/b-jet discrimination will be required to eliminate this background. The Wjj and Zjj backgrounds are much more severe at the LHC/SSC because of the large gluon luminosity. They were eliminated in Ref. [7, 8] by demanding a semileptonic decay of a b quark, with lepton momentum transverse to the b jet of at least 1 GeV, as mentioned above.

The efficiency for detecting a displaced vertex from a b-quark jet is hoped to reach about 30 percent, or 50 percent to detect at least one displaced vertex per $b\bar{b}$ pair. We present in Table 2 the number of signal and background events with at least one displaced vertex for various values of the Higgs-boson mass for 1000 pb^{-1} of integrated luminosity. We assume a one percent misidentification of a light-quark (or gluon) jet as a b jet. The Wjj and Zjj backgrounds, as well as the single-charm background (which we have not included), could be eliminated completely by requiring a double b tag; however, the double-tag efficiency is only 10 percent. The significance of the signal is about the same as with a single tag. Additionally, one can tag b jets using semileptonic decays; however, this has an efficiency of only about 10 percent, with a one percent misidentification of light-quark jets. The number of signal events with at least one displaced vertex for $m_H = 60$–80 GeV may be enough to detect the Higgs boson at the Tevatron, especially if the light-quark-jet misidentification can be reduced below one percent. One should keep in mind that LEP II will have already explored these masses by the time 1000 pb^{-1} is delivered. However, the confirmation of the Higgs boson at the Tevatron would be of interest since both the ZH (similar to LEP II) and WH processes could be detected. A Higgs boson of mass near the Z-boson mass will be difficult to separate from the WZ and ZZ backgrounds. A Higgs boson of mass in excess of the Z-boson mass would require increased integrated luminosity for discovery.

Let us also consider the Higgs-boson signal for 100 pb^{-1} of integrated luminosity. Presently only CDF has a vertex detector, so we apply cuts to simulate their acceptance: $|\eta_b| < 1$, $p_{Tb} > 15$ GeV, $|\eta_e| < 2.5$, $|\eta_\mu| < 1$, $p_{T\ell} > 20$ GeV, $\not{p}_T > 20$ GeV, $|\Delta R_{b\bar{b}}| > 0.7$, $|\Delta R_{b\ell}| > 0.7$. Although the signal-to-background ratio is again of order unity (for the $Wb\bar{b}$ and $Zb\bar{b}$ backgrounds), the number of signal events is only 2/2 for WH/ZH (including the 50 percent single-tag efficiency) for $m_H = 60$ GeV, decreasing to 1/1 for $m_H = 80$ GeV, not enough for discovery.

For $m_H > 140$ GeV, the $H \to WW^{(*)}$ branching ratio becomes significant, and one can consider searching for WH production, followed by leptonic decay of the like-sign W bosons, leading to an isolated like-sign-dilepton plus missing p_T signature. This signal has no irreducible background, and could potentially be used for $m_H = 140$–180 GeV. Unfortunately, the number of events in 1000 pb^{-1} of integrated luminosity is of the order of unity. This signal could be useful for larger integrated luminosity.

[¶]The Wjj and Zjj backgrounds were calculated using the code developed in Ref. [35].

Table 2: Number of signal and background events, per 1000 pb^{-1}, for production of the Higgs boson in association with a weak vector boson, followed by $H \to b\bar{b}$ and $W \to \ell\bar{\nu}$, $Z \to \ell\bar{\ell}, \nu\bar{\nu}$.

m_H (GeV)	WH/ZH	$Wb\bar{b}/Zb\bar{b}$	Wjj/Zjj
60	50/58	60/52	200/200
80	28/35	39/38	140/170
100	15/20	25/26	100/130
120	8/10	17/18	76/97
140	3/3.8	11/13	52/68

The search for the Higgs boson at the Tevatron is challenging, but is matched by the importance of the search. A Higgs boson in the range 80–140 GeV (the so-called intermediate-mass range) is also difficult for the LHC/SSC to discover. Studies at the LHC/SSC usually focus on the rare two-photon decay of the Higgs boson [38, 39]. It might be worthwhile to reconsider the $b\bar{b}$ decay mode at these machines [40, 41].

3 "Bosonic" Higgs

The standard-model Higgs boson is responsible for generating the masses of both the weak vector bosons and the fermions. One can imagine that the mass generation of the weak vector bosons has little or nothing to do with that of the fermions [42, 43, 44, 45, 46, 47, 48]. A Higgs boson associated only with the generation of the weak-vector-boson masses would be expected to have couplings to the weak vector bosons of standard-model strength, but suppressed couplings to fermions. We will refer to such a particle as a "bosonic" Higgs.[‖] For example, a bosonic Higgs can arise in models with two Higgs doublets [42, 43, 45, 46] or with doublets and triplets[**] [49, 47, 48], although fine tuning of the renormalized coupling of the Higgs boson to fermions is necessary in both cases [42, 46, 47, 48]. In general, one expects some mixing to occur such that a bosonic Higgs has a non-vanishing coupling to fermions.

Since the fermionic decay modes of a bosonic Higgs are greatly suppressed, the decay of a bosonic Higgs of mass less than $2M_W$ is not dominated by $H \to b\bar{b}$. It was noted in Refs. [43, 45, 48] that the dominant decay mode of a sufficiently light bosonic Higgs is to two photons via a W-boson loop [50], as shown in Fig. 4(a). The bosonic Higgs can also decay to $b\bar{b}$ at one loop, as shown in Fig. 4(b); however, this decay mode is suppressed relative to the two-photon mode by m_b^2/M_W^2 (assuming the fine tuning mentioned above), and can be neglected. As the Higgs-boson mass approaches M_W, the decay $H \to WW^*$ (and even $H \to W^*W^*$ [51]) begins to compete with the two-photon decay. The branching ratios of a bosonic Higgs to $\gamma\gamma$, $WW^{(*)}$, and $ZZ^{(*)}$ are shown in Fig. 5. Note that a top-quark loop does not contribute to the $\gamma\gamma$ decay of the bosonic Higgs. Charged Higgs bosons (present in multi-

[‖]Such a particle is referred to as a "fermiophobic" Higgs in Ref. [43].

[**]The bosonic Higgs bosons in this model are the H_5 and the $H_1^{0\prime}$.

Higgs models) may contribute, if they are not too heavy; their contribution is suppressed relative to that of the W-boson by $M_W^2/m_{H^\pm}^2$.

A bosonic Higgs of mass less than about 60 GeV would have been seen at LEP via $Z \to Z^* H$, with $H \to \gamma\gamma$ [52]. We will show that the Tevatron, with 100 pb^{-1} of integrated luminosity, can search for the two-photon decay of the bosonic Higgs up to about $m_H = 100$ GeV, prior to the commissioning of LEP II. The production process is the same as in the previous section: $q\bar{q} \to WH, ZH$. The photons from the Higgs decay can serve as the trigger, so we can consider both the leptonic and hadronic decays of the W and Z bosons. We simulate the acceptance of the detector with the cuts listed in Table 3. Decreasing the rapidity coverage of all particles to 1 unit decreases the cross sections by about a factor of two. We show in Fig. 6 the cross sections for WH and ZH, followed by $H \to \gamma\gamma$, for both (a) leptonic (including $Z \to \nu\bar{\nu}$) and (b) hadronic decays of the W and Z. For the hadronic decays, we combine the WH and ZH signals since the assumed two-jet invariant-mass resolution (discussed below) cannot separate the W and Z peaks. We use a machine energy of $\sqrt{s} = 1.8$ TeV throughout this section.

Table 3: Acceptance cuts used in section 3.

$\lvert\eta_\gamma\rvert < 2.5$	$p_{T\gamma} > 10$ GeV
$\lvert\eta_\ell\rvert < 2.5$	$p_{T\ell} > 20$ GeV
$\not{p}_T > 20$ GeV	(for $W \to \ell\bar{\nu}, Z \to \nu\bar{\nu}$)
$\lvert\eta_j\rvert < 2.5$	$p_{Tj} > 15$ GeV
$\lvert\Delta R_{jj}\rvert > 0.7$	$\lvert\Delta R_{j\gamma}\rvert > 0.7$

For the leptonic decay of the W and Z bosons, the main background is $W\gamma\gamma$ [53] and $Z\gamma\gamma$. We assume a photon energy resolution of $\Delta E_\gamma/E_\gamma = .15/\sqrt{E_\gamma} \oplus .01$; this corresponds to a two-photon invariant-mass resolution of approximately $\Delta M_{\gamma\gamma}/M_{\gamma\gamma} = .15/\sqrt{M_{\gamma\gamma}} \oplus .007$. We integrate the background over an invariant-mass bin of $\pm 2\Delta M_{\gamma\gamma}$ centered about m_H, which contains nearly all the signal events. The resulting backgrounds are less than 10^{-4} pb for $m_H > 60$ GeV, too small to display in Fig. 6. There is no background from WZ or ZZ since $Z \to \gamma\gamma$ is forbidden by Yang's theorem [54]. Thus the signal for the bosonic Higgs produced in association with a W or Z which decays leptonically is essentially background free.

The dominant background when the W and Z decay hadronically is a mixed QCD/QED process leading to a $jj\gamma\gamma$ final state [55, 56, 57, 58]. We take a two-jet invariant-mass resolution as in the previous section, $\Delta M_{jj}/M_{jj} = .80/\sqrt{M_{jj}} \oplus .03$, and integrate over a bin of width $\pm 2\Delta M_{jj}$ centered on the W or Z mass; effectively, this corresponds to 65 GeV$< M_{jj} <$ 105 GeV, with no effort made to separate the W and Z peaks. The two-photon invariant-mass bin is treated as above. The resulting cross section is shown in Fig. 6(b). The signal is above the background up to a Higgs-boson mass of about 110 GeV.

Although the bosonic Higgs cannot be produced via gluon fusion, it is produced with standard-model strength via $V^*V^* \to H$ ($V = W, Z$). Because the virtual vector bosons are

radiated from quarks and antiquarks, the final state contains two jets, and thus also has a $jj\gamma\gamma$ signal. This cross section is shown in Fig. 7, with the acceptance cuts listed in Table 3, plus the requirement that the two-jet invariant mass exceed 100 GeV to separate it from the WH/ZH signal. Also shown in Fig. 7 is the $jj\gamma\gamma$ background with the same cuts; the signal lies above the background up to $m_H = 90$ GeV. The two-photon signal without the additional jets lies below the continuum background from $q\bar{q}, gg \to \gamma\gamma$.

We list in Table 4 the number of signal and background events for WH/ZH production for 100 pb^{-1} of integrated luminosity. Table 5 gives the number of signal and background events for the weak-vector-boson-fusion process, also for 100 pb^{-1}. It should be relatively straightforward to search for a bosonic Higgs decaying to two photons up to the point where the two-photon branching ratio falls off, roughly $m_H = 100$ GeV. If such a particle were discovered, it would have dramatic consequences for our understanding of the source of electroweak symmetry breaking.

Table 4: Number of signal and background events, per 100 pb^{-1}, for production of a bosonic Higgs in association with a weak vector boson, followed by $H \to \gamma\gamma$ and $W \to \ell\bar{\nu}$, $Z \to \ell\bar{\ell}, \nu\bar{\nu}$, or $W, Z \to jj$.

m_H (GeV)	WH/ZH (leptonic)	$WH + ZH$ (jets)	$jj\gamma\gamma$
60	14/11	73	5
80	5.3/5	29	2.7
100	0.8/0.7	4.4	1.4

Table 5: Number of signal and background events, per 100 pb^{-1}, for production of a bosonic Higgs via weak-vector-boson fusion, followed by $H \to \gamma\gamma$.

m_H (GeV)	H+ 2 jets	$jj\gamma\gamma$
60	8	4.5
80	4.7	2.7
100	1	1.6

With 1000 pb^{-1}, it may be possible to detect a bosonic Higgs of $m_H > 100$ GeV decaying to WW^* if it is produced in association with a W boson, and the like-sign W's decay leptonically, leading to an isolated like-sign dilepton plus missing p_T signal. There is no irreducible background to this signal. However, the Higgs-boson mass cannot be reconstructed, due to the loss of the neutrinos.

One might also consider the possibility that the Higgs boson associated with the generation of the weak-vector-boson masses is also associated with the top quark, but not with any other fermion ("semi-bosonic"). This is suggested by the fact that the top-quark mass is thought to be of the order of the W and Z masses, and is much heavier than the other known

fermions. Such a Higgs boson might arise in a top-quark condensate model. The dominant decay of such a Higgs boson is to two gluons via a top-quark loop for $m_H = 60$–80 GeV, but it still has a significant branching ratio to two photons. It will be copiously produced via gluon fusion. Since the production cross section is proportional to the $H \to gg$ partial width, the cross section for $gg \to H \to \gamma\gamma$ is proportional to $\Gamma(H \to gg) \times BR(H \to \gamma\gamma) \approx \Gamma(H \to \gamma\gamma)$, i.e., it is independent of $\Gamma(H \to gg)$, and depends only on $\Gamma(H \to \gamma\gamma)$. The cross section for $gg \to H \to \gamma\gamma$ is presented in Fig. 8, with cuts on the photons of $|\eta_\gamma| < 1$ and $p_{T\gamma} > 10$ GeV. The rapidity is restricted to less than unity to suppress the background from $q\bar{q} \to \gamma\gamma$, which is peaked in the forward-backward direction. This background, combined with $gg \to \gamma\gamma$, integrated over an invariant-mass bin of $\pm 2\Delta M_{\gamma\gamma}$ centered on m_H, with $\Delta M_{\gamma\gamma}$ as given previously, is also presented in Fig. 8; it is much larger than the signal.[††] More than 1000 pb^{-1} of integrated luminosity would be needed to establish a signal.

4 Conclusions

We have studied the production and detection of the standard Higgs boson at the Fermilab Tevatron. With 1000 pb^{-1} of integrated luminosity, it may be possible to observe the Higgs boson produced in association with a W or Z, followed by $H \to b\bar{b}$ and $W \to \ell\bar{\nu}$, $Z \to \ell\bar{\ell}, \nu\bar{\nu}$, for $m_H = 60$–80 GeV. Excellent light-quark-jet/b-jet discrimination, and some c-jet/b-jet discrimination, will be required. Higher Higgs-boson masses will require increased integrated luminosity for discovery. Although the search for the Higgs boson at the Tevatron is tantalizing, our study has further strengthened our conviction that a higher-energy collider, such as the LHC or SSC, is needed to explore the electroweak-symmetry-breaking mechanism.

We have also studied the possibility of detecting a non-standard Higgs boson with suppressed couplings to fermions, dubbed the bosonic Higgs, via its enhanced two-photon decay mode. With just 100 pb^{-1} of integrated luminosity, it will be possible to detect such a particle, produced in association with a W or Z, with the weak vector bosons decaying leptonically or hadronically, up to $m_H = 100$ GeV. There may also be an observable signal from the weak-vector-boson-fusion process. The discovery of such a particle would have an enormous impact on our understanding of the electroweak-symmetry-breaking mechanism.

5 Acknowledgements

We are grateful for conversations with B. Blair, E. Boos, S. Dawson, E. Eichten, K. Ellis, S. Errede, G. Forden, S. Geer, H. Gordon, J. Gunion, T. Han, R. Kauffman, S. Kuhlmann, T. LeCompte, R. Lipton, T. Liss, F. Paige, S. Parke, S. Protopopescu, C. Quigg, A. White, and J. Yoh. This work was supported under contract no. DE-AC02-76CH00016 with the U.S. Department of Energy.. S.W. thanks the Aspen Center for Physics where part of this work was performed. S.W. was partially supported by the Texas National Research Laboratory Commission.

[††]We have not included the QCD correction to $q\bar{q} \to \gamma\gamma$, which is given in Ref. [59].

References

[1] ALEPH Collaboration, Phys. Rep. **216**, 253 (1992); DELPHI Collaboration, P. Abreu *et al.*, Nucl. Phys. **B373**, 3 (1992); L3 Collaboration, O. Adriani *et al.*, Phys. Lett. **303B**, 391 (1993); CERN-PPE/93-30 (1993); OPAL Collaboration, M. Akrawy *et al.*, Phys. Lett. **253B**, 511 (1991).

[2] S. L. Wu *el al.*, in *Proceedings of the ECFA Workshop on LEP 200*, Aachen, 1986, eds. A. Böhm and W. Hoogland, CERN 87-08, Vol. II, p. 312.

[3] For a review, see J. Gunion, H. Haber, G. Kane, and S. Dawson, *The Higgs Hunter's Guide* (Addison-Wesley, New York, 1990).

[4] S. Glashow, D. Nanopoulos, and A. Yildiz, Phys. Rev. D **18**, 1724 (1978).

[5] L. Poggioli, in *Proceedings of the ECFA Large Hadron Collider Workshop*, Aachen, 1990, eds. G. Jarlskog and D. Rein, CERN 90-10, Vol. II, p. 547.

[6] J. Gunion, P. Kalyniak, M. Soldate, and P. Galison, Phys. Rev. Lett. **54**, 1226 (1985); Phys. Rev. D **34**, 101 (1986).

[7] F. Gilman and L. Price, in *Proc. of the 1986 Summer Study on the Physics of the Superconducting Supercollider*, Snowmass, CO, eds. R. Donaldson and J. Marx, p. 185.

[8] J. Brau, K. Pitts, and L. Price, in *Proc. of the Summer Study on High Energy Physics in the 1990's*, Snowmass, CO, ed. S. Jensen (World Scientific, Singapore, 1989), p. 103.

[9] J. Gunion and G. Kane, in *Research Directions for the Decade, Proc. of the 1990 Summer Study on High Energy Physics*, Snowmass, CO, ed. E. Berger (World Scientific, Singapore, 1992), p. 59.

[10] P. Agrawal and S. Ellis, Phys. Lett. **229B**, 145 (1989).

[11] H. Georgi, S. Glashow, M. Machacek, and D. Nanopoulos, Phys. Rev. Lett. **40**, 692 (1978).

[12] R. Cahn and S. Dawson, Phys. Lett. **136B**, 196 (1984); G. Kane, W. Repko, and W. Rolnick, Phys. Lett. **148B**, 367 (1984).

[13] D. Dicus and S. Willenbrock, Phys. Rev. D **39**, 751 (1989).

[14] J. Ng and P. Zakarauskas, Phys. Rev. D **29**, 876 (1984).

[15] Z. Kunszt, Nucl. Phys. **B247**, 339 (1984).

[16] P. Harriman, A. Martin, R. Roberts, and W. J. Stirling, Phys. Rev. D **42**, 798 (1990).

[17] S. Dawson, Nucl. Phys. **B359**, 283 (1991); A. Djouadi, M. Spira, and P. Zerwas, Phys. Lett. **264B**, 440 (1991).

[18] D. Graudenz, M. Spira, and P. Zerwas, Phys. Rev. Lett. **70**, 1372 (1993).

[19] S. Dawson and R. Kauffman, private communication.

[20] T. Han and S. Willenbrock, Phys. Lett. **273B**, 167 (1990); J. Ohnemus and W. J. Stirling, Phys. Rev. D **47**, 2722 (1993); H. Baer, B. Bailey, and J. Owens, Phys. Rev. D **47**, 2730 (1993).

[21] T. Han, G. Valencia, and S. Willenbrock, Phys. Rev. Lett. **69**, 3274 (1992).

[22] T. Rizzo, Phys. Rev. D **22**, 722 (1980); W.-Y. Keung and W. Marciano, Phys. Rev. D **30**, 248 (1984).

[23] M. Golden, in *Physics at Fermilab in the 1990's*, Breckenridge, CO, eds. D. Green and H. Lubatti (World Scientific, Singapore, 1990), p. 112.

[24] R. K. Ellis, I. Hinchliffe, M. Soldate, and J. van der Bij, Nucl. Phys. **B297**, 221 (1988).

[25] CDF Collaboration, F. Abe *et al.*, Phys. Rev. D **41**, 1717 (1990).

[26] V. Barger, A. Stange, and R. Phillips, Phys. Rev. D **45**, 1484 (1992).

[27] M. Mangano, IFUP-TH-36-92 (1992).

[28] A. Ballestrero and E. Maina, Phys. Lett. **287B**, 231 (1992).

[29] J. Ohnemus, Phys. Rev. D **44**, 3477 (1991); S. Frixione, P. Nason, and G. Ridolfi, Nucl. Phys. **B383**, 3 (1992).

[30] J. Ohnemus and J. Owens, Phys. Rev. D **43**, 3626 (1991); B. Mele, P. Nason, and G. Ridolfi, Nucl. Phys. **B357**, 409 (1991).

[31] S. Ellis, R. Kleiss, and W. J. Stirling, Phys. Lett. **154B**, 435 (1985); **163B**, 261 (1985); R. Kleiss and W. J. Stirling, Nucl. Phys. **B262**, 235 (1985); Phys. Lett. **180B**, 171 (1986).

[32] J. Gunion, Z. Kunszt, and M. Soldate, Phys. Lett. **163B**, 389 (1985); **168B**, 427(E) (1986); J. Gunion and M. Soldate, Phys. Rev. D **34**, 826 (1986).

[33] R. K. Ellis and R. Gonsalves, in *Supercollider Physics, Proceedings of the Oregon Workshop on Super High Energy Physics*, 1985, ed. by D. Soper (World Scientific, Singapore, 1986), p. 287.

[34] P. Arnold and M. H. Reno, Nucl. Phys. **B319**, 37 (1989); R. Gonsalves, J. Pawlowski, and C.-F. Wai, Phys. Rev. D **40**, 2245 (1989).

[35] V. Barger, T. Han, J. Ohnemus, and D. Zeppenfeld, Phys. Rev. Lett. **62**, 1971 (1989); Phys. Rev. D **40**, 2888 (1989); D **41**, 1715(E) (1990).

[36] F. Berends, W. Giele, H. Kuijf, R. Kleiss, and W. J. Stirling, Phys. Lett. **224B**, 237 (1989).

[37] M. Mangano and S. Parke, Phys. Rev. D **41**, 59 (1990).

[38] See the *Proceedings of the ECFA Large Hadron Collider Workshop*, Aachen, 1990, eds. G. Jarlskog and D. Rein, CERN 90-10.

[39] See the SDC Technical Design Report, SDC-92-201 (1992); GEM Technical Design Report, GEM-TN-93-262 (1993).

[40] T. Garavaglia, W. Kwong, and D.-D. Wu, PVAM-HEP-93-1 (1993).

[41] J. Dai, J. Gunion, and R. Vega, SLAC-PUB-6265 (1993).

[42] H. Haber, G. Kane, and T. Sterling, Nucl. Phys. **B161**, 493 (1979).

[43] T. Weiler, in *Collider Physics: Current Status and Future Prospects*, Proceedings of the Eighth Vanderbilt International Conference on High Energy Physics, Nashville, Tennessee, 1987, edited by J. Brau and R. Panvini (World Scientific, Singapore, 1988), p. 219; H. Pois, T. Weiler and T. C. Yuan, Phys. Rev. D **47**, 3886 (1993).

[44] M. Berger and M. Chanowitz, Phys. Rev. Lett. **68**, 757 (1992).

[45] V. Barger, N. Deshpande, J. Hewett, and T. Rizzo, OITS-499 (1992).

[46] J-L. Basdevant, E. Berger, D. Dicus, C. Kao, and S. Willenbrock, Phys. Lett. **313B**, 402 (1993).

[47] J. Gunion, R. Vega, and J. Wudka, Phys. Rev. D **42**, 1673 (1990); **43**, 2322 (1991).

[48] P. Bamert and Z. Kunszt, Phys. Lett. **306B**, 335 (1993).

[49] H. Georgi and M. Machacek, Nucl. Phys. **B262**, 463 (1985); M. Chanowitz and M. Golden, Phys. Lett. **165B**, 105 (1985).

[50] A. Vainshtein, M. Voloshin, V. Zakharov, and M. Shifman, Yad. Fiz. **30**, 1368 (1979) [Sov. J. Nucl. Phys. **30**, 711 (1979)].

[51] V. Barger, G. Bhattacharya, T. Han, and B. Kniehl, Phys. Rev. D **43**, 779 (1991).

[52] ALEPH Collaboration, D. Buskulic *et al.*, Phys. Lett. **308B**,425 (1993); L3 Collaboration, O. Adriani *et al.*, Phys. Lett. **295B**, 337 (1992); CERN-PPE/93-31 (1993); OPAL Collaboration, P. Acton *et al.*, Phys. Lett. **311B**, 391 (1993).

[53] R. Kleiss, Z. Kunszt, and W. J. Stirling, Phys. Lett. **253B**, 269 (1991); J. Ohnemus and W. J. Stirling, Phys. Rev. D **47**, 336 (1992).

[54] C. N. Yang, Phys. Rev. **77**, 242 (1950).

[55] F. Berends *et al.*, Nucl. Phys. **B264**, 243 (1986); **B264**, 265 (1986).

[56] J. Gunion and Z. Kunszt, Phys. Lett. **159B**, 167 (1985); **176B**, 477 (1986).

[57] M. Mangano and S. Parke, Nucl. Phys. **B299**, 673 (1988).

[58] V. Barger, T. Han, D. Zeppenfeld, and J. Ohnemus, Phys. Rev. D **41**, 2782 (1990).

[59] P. Aurenche, R. Baier, A. Douiri, M. Fontannaz, and D. Schiff, Z. Phys. C **29**, 459 (1985); B. Bailey, J. Owens, and J. Ohnemus, Phys. Rev. D **46**, 2018 (1992).

6 Figure Captions

Fig. 1 - Cross sections for various Higgs-boson production processes at the Tevatron ($\sqrt{s} = 2$ TeV) versus the Higgs-boson mass. The HMRSB parton distribution functions [16] are used for all calculations, and $m_t = 150$ GeV is assumed.

Fig. 2 - Branching ratios of the standard Higgs boson into $b\bar{b}$, $c\bar{c}$, $\tau^+\tau^-$, $WW^{(*)}$, and $ZZ^{(*)}$, versus the Higgs-boson mass.

Fig. 3 - Cross sections and backgrounds for a.) WH and b.) ZH production, followed by $H \to b\bar{b}$ and $W \to \ell\bar{\nu}$, $Z \to \ell\bar{\ell}, \nu\bar{\nu}$, versus the Higgs-boson mass. The cuts which have been made to simulate the acceptance of the detector are listed in Table 1. The backgrounds are from $Wb\bar{b}$ and $Zb\bar{b}$, WZ and ZZ followed by $Z \to b\bar{b}$, and $t\bar{t} \to W^+W^-b\bar{b}$ with one W missed (for WH) or with both W's missed (for ZH, $Z \to \nu\bar{\nu}$).

Fig. 4 a.) Two-photon decay of a bosonic Higgs via a W-boson loop; b.) Decay of a bosonic Higgs to $b\bar{b}$ via virtual W and Z bosons. The latter decay mode is suppressed relative to the former by m_b^2/M_W^2.

Fig. 5 - Branching ratios of a bosonic Higgs to $\gamma\gamma$, $WW^{(*)}$, and $ZZ^{(*)}$, versus the Higgs-boson mass.

Fig. 6 - Cross sections and backgrounds for the bosonic Higgs, produced in association with a W or Z, followed by $H \to \gamma\gamma$ and (a) $W \to \ell\bar{\nu}$, $Z \to \ell\bar{\ell}, \nu\bar{\nu}$, and (b) $W, Z \to jj$, versus the Higgs-boson mass. The cuts which have been made to simulate the acceptance of the detector are listed in Table 3. The signal with the leptonic decay of the weak vector bosons has no background. The background to the hadronic decay is from a mixed QED/QCD process leading to a $jj\gamma\gamma$ final state.

Fig. 7 - Cross section and background for the production of the bosonic Higgs via weak-vector-boson fusion, followed by $H \to \gamma\gamma$, versus the Higgs-boson mass. The cuts which have been made to simulate the acceptance of the detector are listed in Table 3. The two jets in the final state, left over from the radiation of the weak vector bosons, have an invariant mass greater than 100 GeV. The background is from a mixed QED/QCD process leading to a $jj\gamma\gamma$ final state.

Fig. 8 - Cross section and background for the production of the top-quark-condensate Higgs boson, followed by the decay $H \to \gamma\gamma$, versus the Higgs-boson mass. The background is from $q\bar{q}, gg \to \gamma\gamma$.

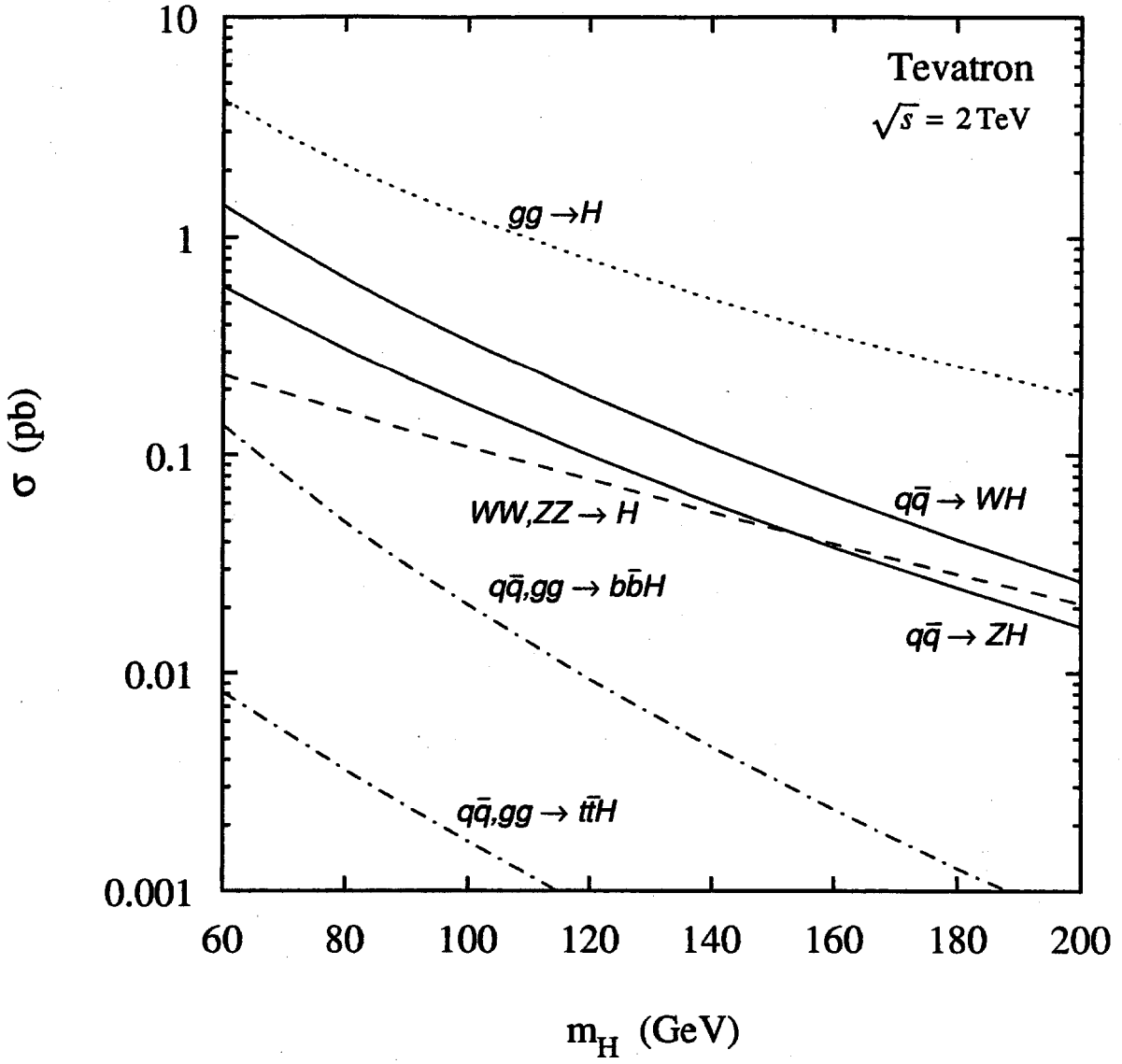
Tevatron
$\sqrt{s}$ = 2 TeV
$gg \to H$
$q\bar{q} \to WH$
$WW,ZZ \to H$
$q\bar{q},gg \to b\bar{b}H$
$q\bar{q} \to ZH$
$q\bar{q},gg \to t\bar{t}H$
σ (pb)
10
1
0.1
0.01
0.001
60
80
100
120
140
160
180
200
m_H (GeV)

Figure 1

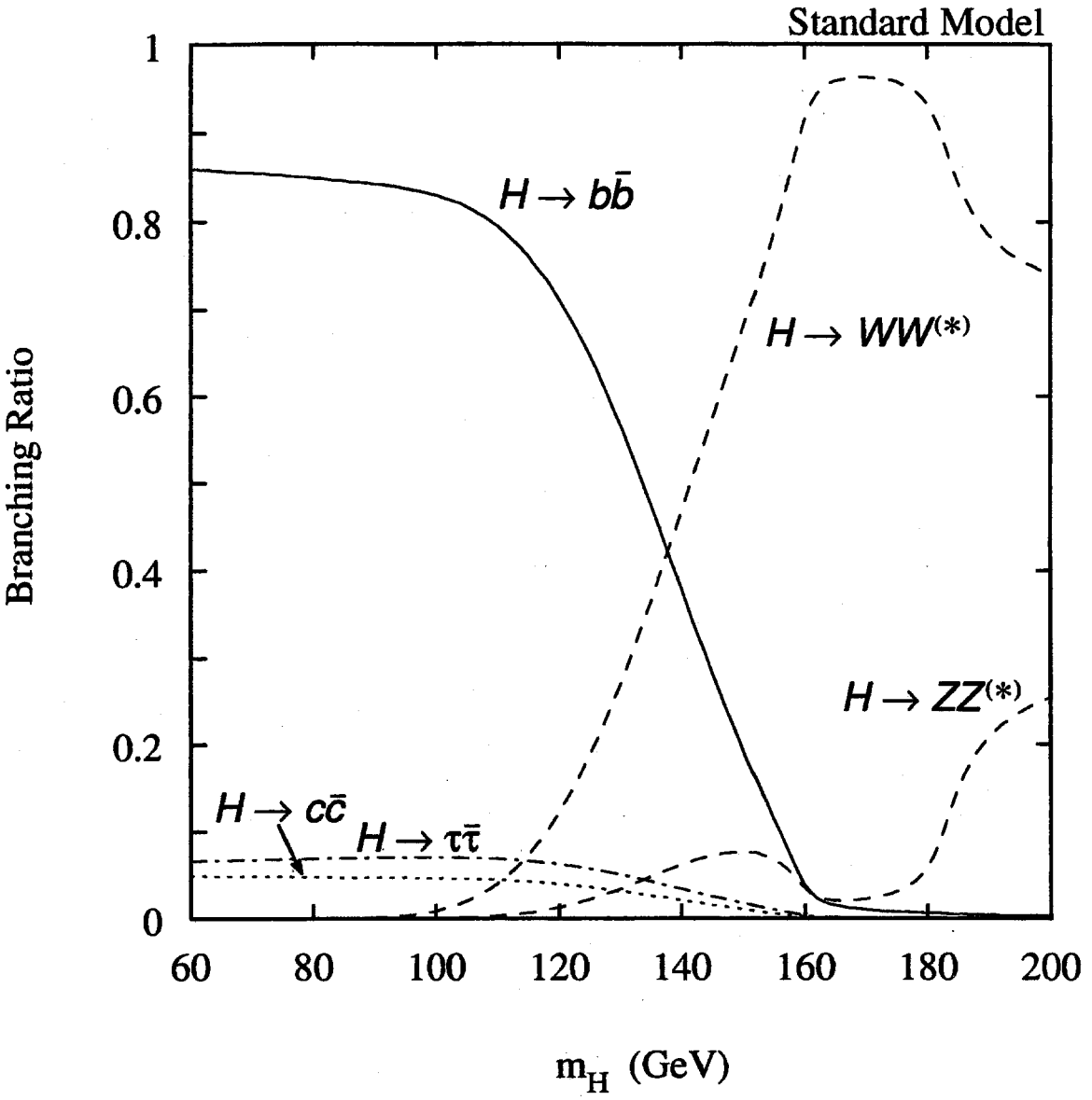
Standard Model
Branching Ratio
1
0.8
0.6
0.4
0.2
0
$H \to b\bar{b}$
$H \to WW^{(*)}$
$H \to ZZ^{(*)}$
$H \to c\bar{c}$
$H \to \tau\bar{\tau}$
60
80
100
120
140
160
180
200
m_H (GeV)

Figure 2

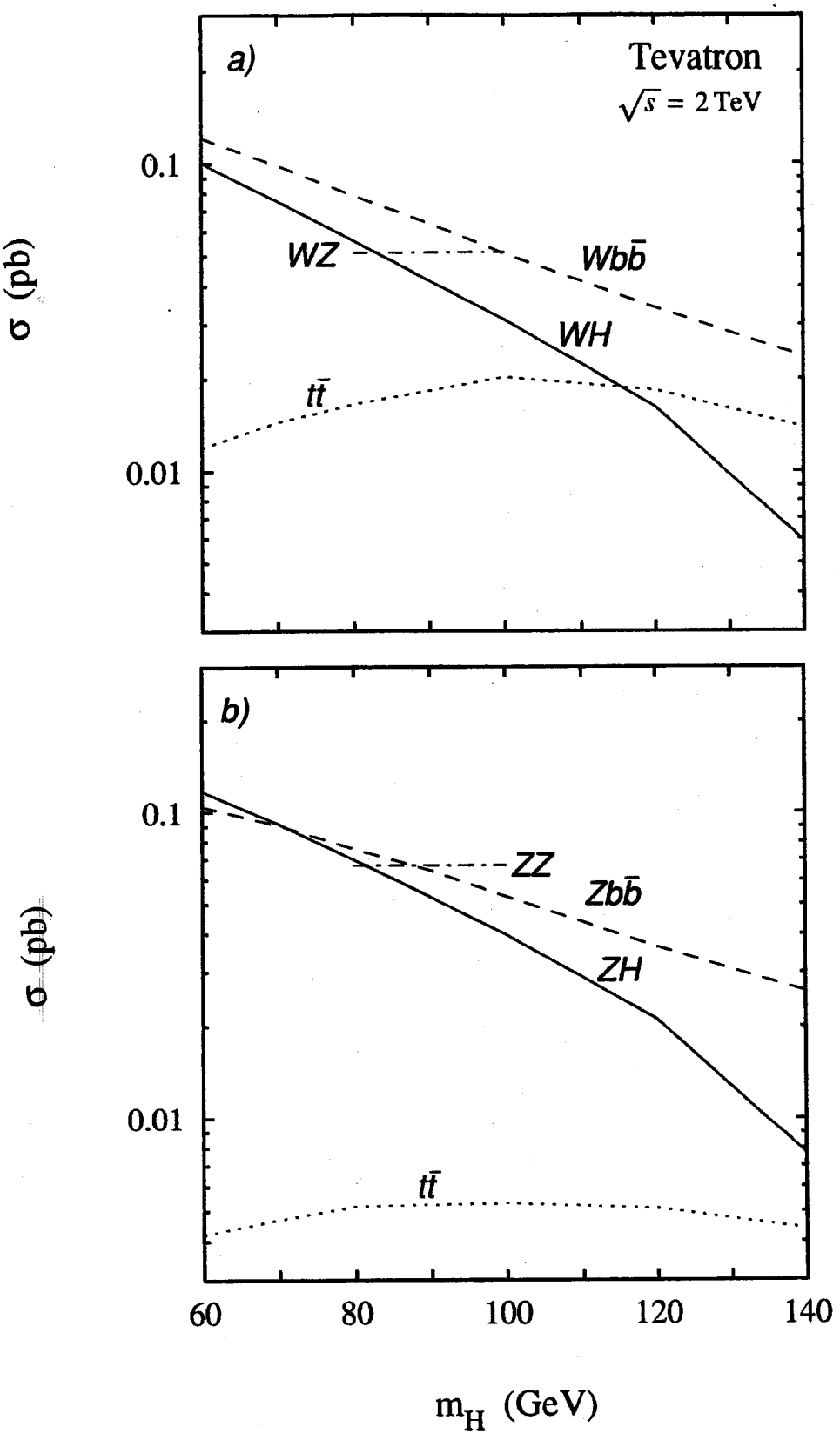
a)
Tevatron
$\sqrt{s}$ = 2 TeV
0.1
0.01
σ (pb)
WZ
Wbb̄
WH
tt̄
b)
0.1
0.01
σ (pb)
ZZ
Zbb̄
ZH
tt̄
60
80
100
120
140
m_H (GeV)

Figure 3

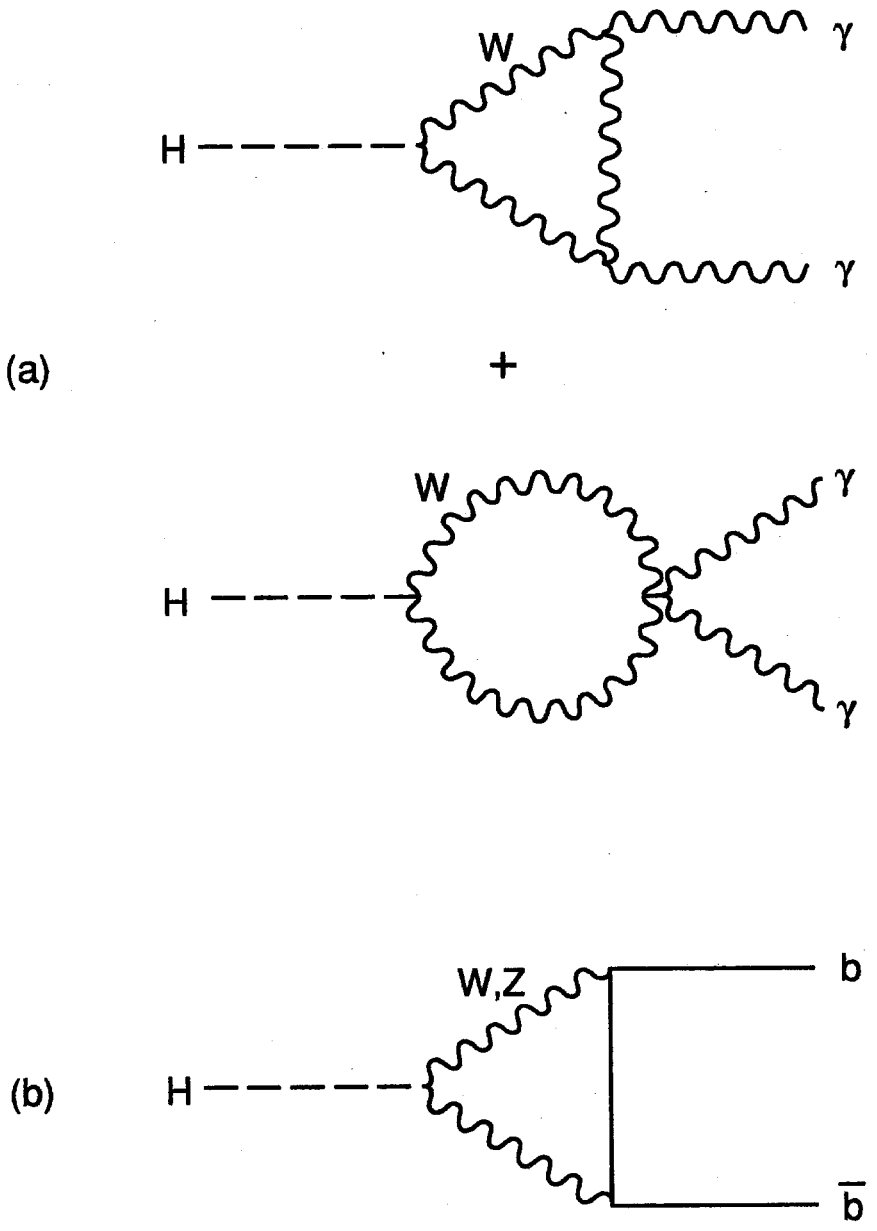

Figure 4

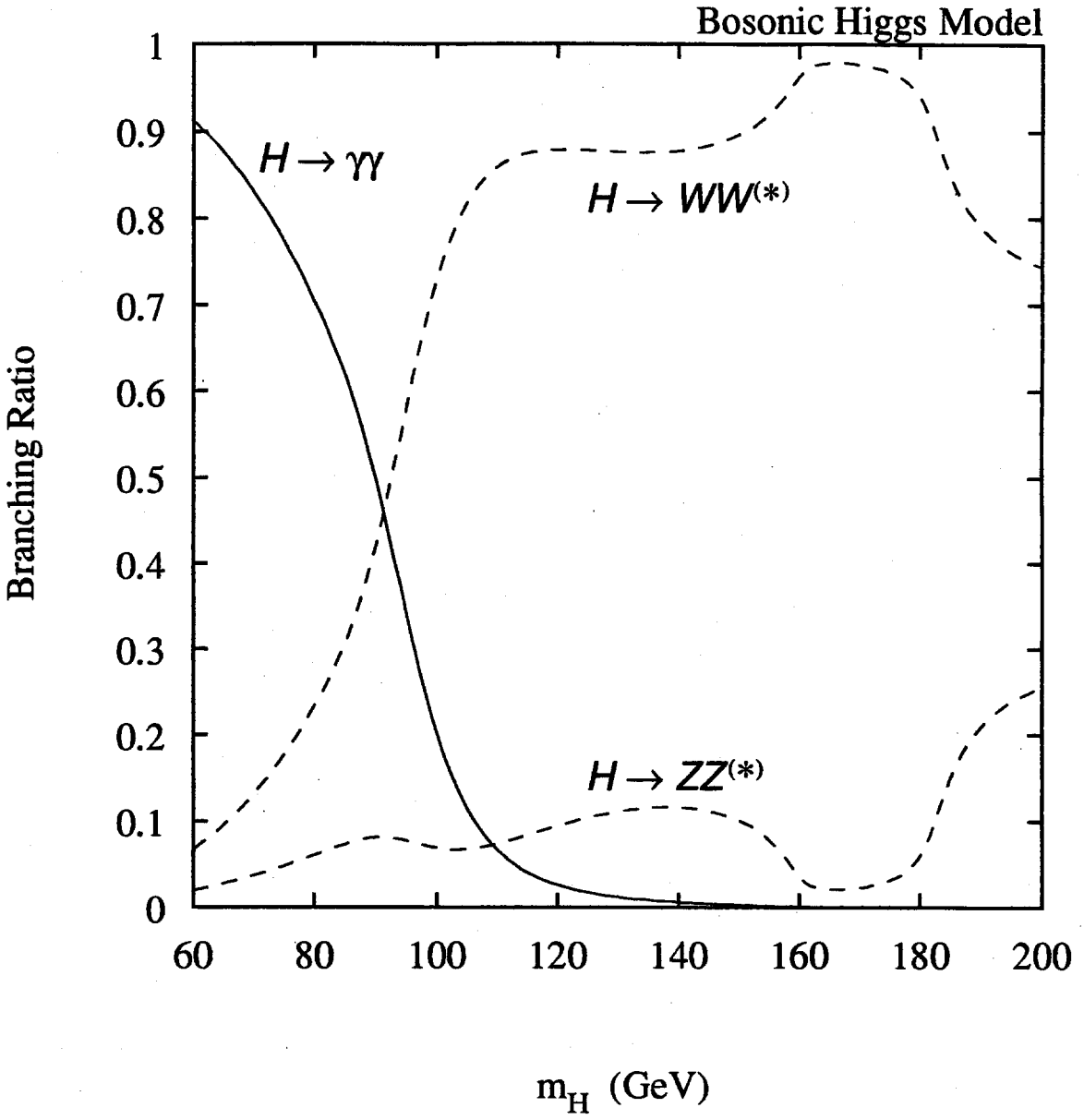
Bosonic Higgs Model
Branching Ratio
1
0.9
0.8
0.7
0.6
0.5
0.4
0.3
0.2
0.1
0
60
80
100
120
140
160
180
200
$H \to \gamma\gamma$
$H \to WW^{(*)}$
$H \to ZZ^{(*)}$
m_H (GeV)

Figure 5

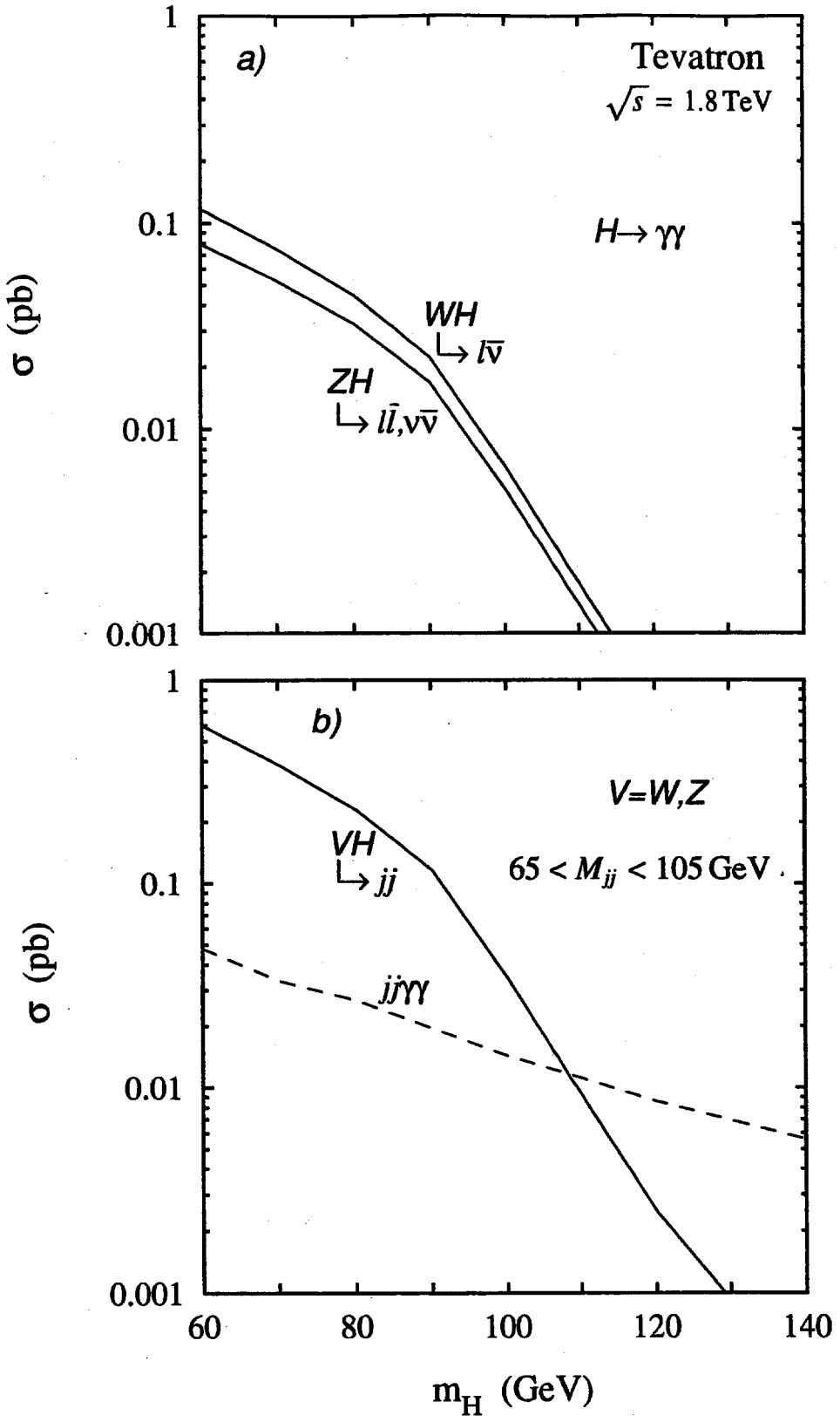
a)
Tevatron
$\sqrt{s}$ = 1.8 TeV
$H \to \gamma\gamma$
WH
$\hookrightarrow l\bar{\nu}$
ZH
$\hookrightarrow l\bar{l}, \nu\bar{\nu}$
σ (pb)
1
0.1
0.01
0.001
b)
V=W,Z
65 < M_{jj} < 105 GeV
VH
$\hookrightarrow jj$
$jj\gamma\gamma$
σ (pb)
1
0.1
0.01
0.001
60
80
100
120
140
m_H (GeV)

Figure 6

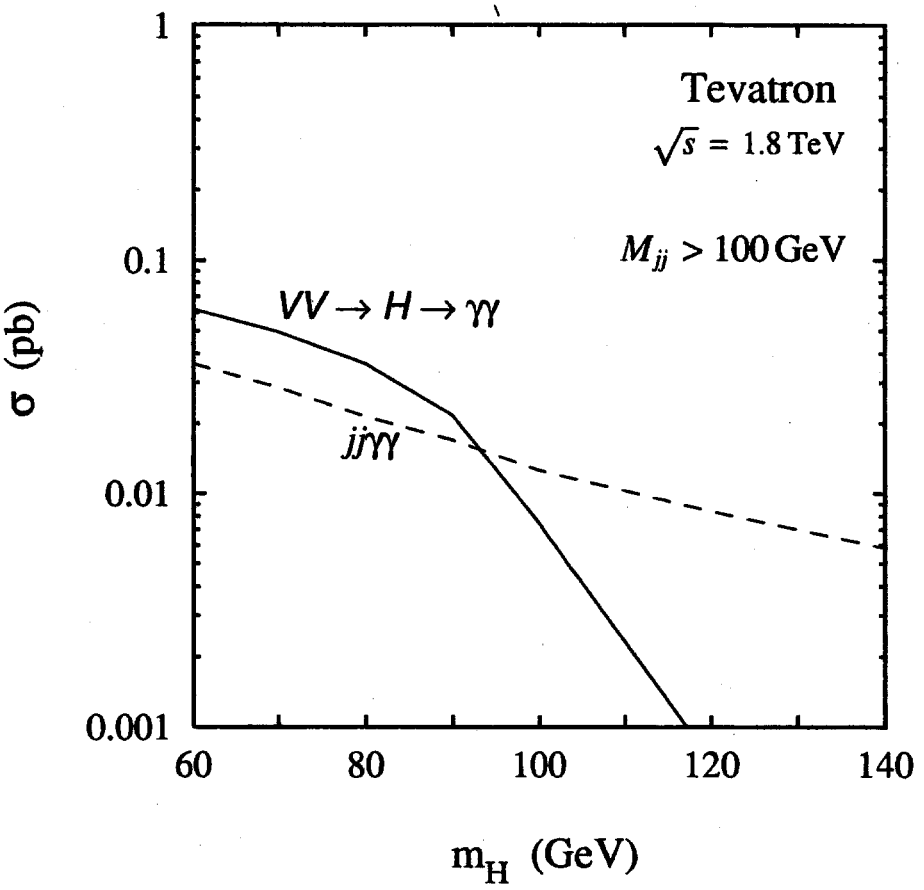
Tevatron
$\sqrt{s}$ = 1.8 TeV
M_{jj} > 100 GeV
$VV \rightarrow H \rightarrow \gamma\gamma$
$jj\gamma\gamma$
σ (pb)
1
0.1
0.01
0.001
60
80
100
120
140
m_H (GeV)

Figure 7

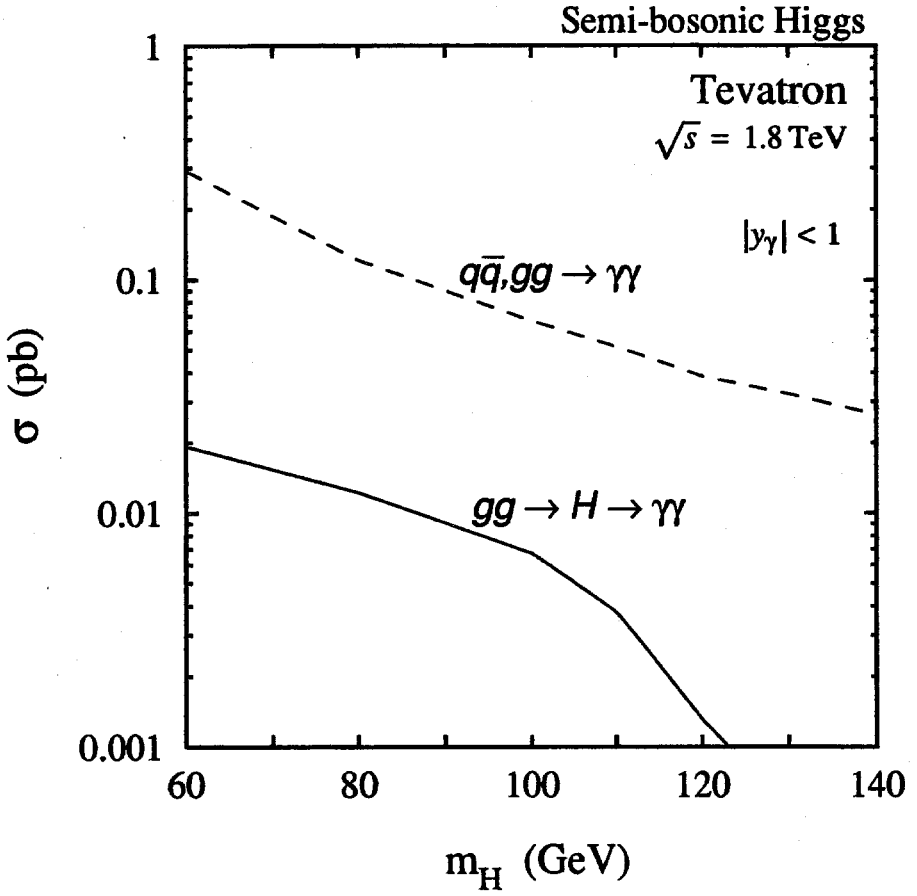
Semi-bosonic Higgs
Tevatron
$\sqrt{s}$ = 1.8 TeV
$|y_\gamma| < 1$
$q\bar{q},gg \rightarrow \gamma\gamma$
$gg \rightarrow H \rightarrow \gamma\gamma$
σ (pb)
1
0.1
0.01
0.001
60
80
100
120
140
m_H (GeV)

Figure 8